How climate, migration ability and habitat fragmentation affect the projected future distribution of European beech

FRÉDÉRIK SALTRÉ[1,2], ANNE DUPUTIÉ[1,3], CÉDRIC GAUCHEREL[4] and ISABELLE CHUINE[1]

[1]*CEFE UMR 5175, CNRS - Université de Montpellier - Université Paul-Valéry Montpellier – EPHE, 1919 route de Mende, 34293 Montpellier Cedex 05, France,* [2]*The Environment Institute, School of Earth and Environmental Science, The University of Adelaide, Adelaide, South Australia 5005, Australia,* [3]*Laboratoire Génétique et Evolution des Populations Végétales, CNRS UMR 8198, Université Lille1 – Sciences et Technologies, Villeneuve d'Ascq Cedex F-59655, France,* [4]*French Institute of Pondicherry, IFP-CNRS, Pondicherry 605 001, India*

Abstract

Recent efforts to incorporate migration processes into species distribution models (SDMs) are allowing assessments of whether species are likely to be able to track their future climate optimum and the possible causes of failing to do so. Here, we projected the range shift of European beech over the 21st century using a process-based SDM coupled to a phenomenological migration model accounting for population dynamics, according to two climate change scenarios and one land use change scenario. Our model predicts that the climatically suitable habitat for European beech will shift north-eastward and upward mainly because (i) higher temperature and precipitation, at the northern range margins, will increase survival and fruit maturation success, while (ii) lower precipitations and higher winter temperature, at the southern range margins, will increase drought mortality and prevent bud dormancy breaking. Beech colonization rate of newly climatically suitable habitats in 2100 is projected to be very low (1–2% of the newly suitable habitats colonised). Unexpectedly, the projected realized contraction rate was higher than the projected potential contraction rate. As a result, the realized distribution of beech is projected to strongly contract by 2100 (by 36–61%) mainly due to a substantial increase in climate variability after 2050, which generates local extinctions, even at the core of the distribution, the frequency of which prevents beech recolonization during more favourable years. Although European beech will be able to persist in some parts of the trailing edge of its distribution, the combined effects of climate and land use changes, limited migration ability, and a slow life-history are likely to increase its threat status in the near future.

Keywords: climate change, demography, *Fagus sylvatica*, Gibbs-based migration model, habitat fragmentation, migration lag, process-based species distribution model

Received 23 January 2014; revised version received 14 September 2014 and accepted 29 September 2014

Introduction

Many species are already shifting their range and/or changing their phenology in response to human induced environmental changes (Walther *et al.*, 2002; Cleland *et al.*, 2012) and these effects are projected to increase in the near future (Thomas *et al.*, 2004; Morin *et al.*, 2008, 2009). However, understanding which factors constrain species distributions and restrict their shifts remains a strong challenge (Beale & Lennon, 2012), partly because most models focus on a long-term climate-driven habitat suitability (Schurr *et al.*, 2012; Fordham *et al.*, 2013a) and fail to account for important demographic and evolutionary mechanisms that causing a disequilibrium between vegetation and climate, and potentially increasing extinction risks (Barve *et al.*, 2011; Fordham *et al.*, 2013c).

Although environmental conditions, and primarily climate, determine the region where a species is able to establish populations in the absence of competitors and other negatively interacting species (Holt *et al.*, 1997; Pulliam, 2000), two other major factors control species' range shifts (Peterson *et al.*, 2011). First, species' dispersal rate determines its ability to track climatically suitable areas through time, and accessible geographic regions within a given time span. Limited migration rate can cause disequilibrium between the potential (climatically suitable) and the realized (climatically suitable and accessible) distribution of the species (Normand *et al.*, 2011; Saltré *et al.*, 2013). Second, biotic interactions and perturbations (mostly land use at regional scale) determine the geographic regions where populations of the species can establish and survive (Sala *et al.*, 2000, Thomas *et al.*, 2004; Thuiller *et al.*, 2005). The interplay of climate suitability, migration ability, and

biotic interactions defines the regions that are both accessible and suitable for a given species (Peterson *et al.*, 2011).

The migration rate of many species is much lower than current and future (projected) climate velocity (Pounds *et al.*, 1999; Kremer *et al.*, 2012). In addition, in many modern landscapes, human-driven habitat fragmentation has generated new artificial barriers to species migration that dramatically reduce realized migration rates (Malanson & Armstrong, 1996; Collingham & Huntley, 2000). Climate change, in conjunction with habitat destruction and fragmentation, is thus expected to strongly affect species distributions and extinction risk (Pereira *et al.*, 2010; Fordham *et al.*, 2012). Therefore, accounting for the interplay between climate, migration processes and habitat fragmentation on projections of species distribution is crucial for understanding the circumstances limiting species range shifts.

Species distribution models (SDMs) have often been used to assess factors limiting species distribution. Several types of species distribution models exist (Dormann *et al.*, 2012), spanning from purely correlative models (Guisan & Zimmermann, 2000) to process-based models (Chuine & Beaubien, 2001; Kearney & Porter, 2009). SDMs have been coupled to process-based models of metapopulation dynamics and dispersal processes to more closely approximate species' realized niche and simulate its spatial dynamics (Meier *et al.*, 2012; Fordham *et al.*, 2013a,c). Such coupled models have shown that dispersal, biotic and others factors such as life history or forest fragmentation, might limit many mid- to late- successional species in tracking their climate optimum (Meier *et al.*, 2012). Recently, more complex dynamic models have been developed, incorporating demographic and biotic responses to environmental changes (Dullinger *et al.*, 2012; Pagel & Schurr, 2012; Fordham *et al.*, 2013b; Snell *et al.*, 2014). Although these new methods showed a strong potential to address new questions related to range dynamics (Dullinger *et al.*, 2012), the respective impacts of climate, migration abilities and human-driven landscape fragmentation on species range shift at a regional scale remain far from certain (but see Meier *et al.*, 2011).

Here, we address this general challenge for European beech (*Fagus sylvatica* L.), a widespread forest tree. We coupled a process-based SDM (Chuine & Beaubien, 2001) to a simple demographic model and a phenomenological (i.e. not mechanistic) migration model based on Gibbs point processes that takes into account both dispersal and intra-specific competition processes (Saltré *et al.*, 2009). This model combination has previously shown to accurately predict European beech post-glacial migration routes and spread rate during the last 12 000 years (Saltré *et al.*, 2013). More specifically, we simulated the future distribution of European beech using two climate change scenarios and one land use change scenario for the 21st century, to answer the following questions: Which abiotic factors and ecological processes limit the future habitat suitability of European beech? How do population dynamics, migration, and human-driven landscape changes interplay in determining beech range shifts and migration rate?

Material and methods

We used the process-based SDM PHENOFIT to simulate habitat suitability of European beech (*Fagus sylvatica* L.) under two climate scenarios A1Fi and B2, one of them (A1Fi) coupled (or not) with the land use scenario GRAS, considering either unlimited migration or realistic migration simulated by the Gibbs migration model for the period 1981–2100. This resulted in 6 different simulations (see Table S2 in Section S6). We then overlaid demography and migration (annually simulated using the Gibbs-based migration model, Saltré *et al.*, 2009) over habitat suitability dynamically at a spatial resolution of 5 km × 5 km, to estimate beech realized distribution by 2081–2100 (20-years mean).

Modelling habitat suitability with PHENOFIT

Model overview. The SDM PHENOFIT (Chuine & Beaubien, 2001) is a forward process-based model that estimates the two major components of fitness of temperate tree species, i.e. annual survival and annual reproductive success, as a function of abiotic conditions. The fitness estimated can be used as a proxy of the probability of presence of the species. PHENOFIT has been validated for 25 North American and European tree species (Morin *et al.*, 2007; Gritti *et al.*, 2013). The model estimates the annual reproductive success (probability to produce viable seeds by the end of the annual cycle as function of climate conditions, see details in Chuine & Beaubien, 2001) and the probability of survival, based on the precise phenology (dates of leaf unfolding, flowering, fruit maturation, leaf senescence) in response to local climatic conditions and on its resistance to abiotic stresses such as frost and drought. Compared to the version used by Gritti *et al.* (2013), we estimate leaf senescence date using the approach used by Delpierre *et al.* (2009). The estimate of the annual fitness is defined as the product of the annual survival probability and the annual reproductive success.

The assumptions of the version of the model used for this study are that (i) phenology is a very important driver of reproductive output (Chuine, 2010); (ii) phenology is primarily driven by climatic constraints (Cleland *et al.*, 2007); (iii) tree survival depends upon its ability to resist to climatic stresses such as drought, frost, and repeated failure to photosynthesize enough. The model assumes no demography since it simulates one average adult individual. The model can, however, incorporate local adaptation, by considering different phenological

response curves to climate fitted on phenological data from different provenances.

PHENOFIT requires as inputs the daily minimum, mean and maximum temperatures, monthly or daily precipitation, and soil water holding capacity, and outputs yearly estimates for phenology, leaf area index, reproductive success, survival, and fitness, at the same spatial resolution as the inputs.

Environmental data. We simulated beech habitat suitability under (i) current European climate conditions, observed between 1981 and 2000; (ii) projected climatic conditions under two scenarios of greenhouse gas emission, for the period 2001–2100 (A1Fi and B2).

Climate data (minimum, mean and maximum monthly temperatures, monthly precipitations) were obtained at a 10′ resolution. Current climate data are combined data of CRU TS2.1 data and CRU CL2.2 data (Mitchell & Jones, 2005). Climate projections for scenarios A1Fi and B2 (closest to RCP8.5 and RCP6 scenarios respectively, Rogelj *et al.*, 2012) under the general circulation model HadCM3 (Hadley Centre, Oxford, United Kingdom, Gordon *et al.*, 2000) were obtained from the ATEAM project (Mitchell *et al.*, 2004). These data are monthly mean values corrected by their anomalies on the benchmark period (1961–1990, 30-years mean climate data). Because daily climate data are needed to run PHENOFIT and derive habitat suitability, we used a stochastic climate generator to create daily temperature (Nicks *et al.*, 1995; Morin & Chuine, 2005).

The ALARM scenario GRAS, downscaled by Meier *et al.* (2012), provided the land use scenario (indicating the presence or absence of forests in each 10′ pixel) for 2020, 2050 and 2080. These data are intermediate land use maps between 2020, 2050 and 2080 every 10 years by randomly removing and adding a fraction of disappearing and appearing forested pixels. Soil water holding capacity data were taken from Webb *et al.* (2000).

Model parameterization. The parameters of the sub-models of PHENOFIT describing resistance to frost, drought, and the timing of the different phenological events were obtained from empirical data. The frost and drought resistance sub-models of PHENOFIT were parameterized using data from the literature; either issued from expert assessment or from experiments (see Supporting Information, SI). The phenological sub-models determining the dates of budburst, flowering, fruit maturation and leaf senescence were calibrated using time-series of phenological observations recorded in natural populations across the range, together with daily temperature records of the closest meteorological station (see SI Section S1 for details).

Local adaptation. To account for local adaptation of the reaction norms of phenological events to temperature and photoperiod, we parameterized models for nine different provenance regions found in climatically distinct regions across Europe (Figure S1 in Section S1). PHENOFIT was then run for each of the nine parameters sets (one for each provenance region). The nine simulations were then aggregated as follows:

for each pixel, (i) we averaged PHENOFIT's yearly outputs for the three closest calibration regions after weighting them by the inverse of their geographic distance to the pixel; and (ii) averaged these aggregated yearly outputs over 20 years (1981–2000 or 2081–2100) to obtain the mean projected fitness for each pixel, reflecting its suitability for beech survival and reproduction. The assumption behind this is that the nine responses shown by the nine geographic provenances differ and, like many quantitative traits, phenological response curves to climate variables probably vary continuously across space (SI Section S1 and Figure S1). Note that, since there is currently no demography in the model PHENOFIT, we were unable to assess phenotypic changes due to varying selective pressures. How microevolution affects our results is not assessed here.

Habitat suitability. From the fitness map, we determined a fitness threshold, below which beech was considered as 'absent'. This threshold method is commonly used to transform continuous probabilities of presence to presence/absence data in species distribution models (see for review Nenzen & Araújo, 2011). This threshold was calculated by maximizing the sum of sensitivity (proportion of correctly identified actual positives) and specificity (proportion of correctly identified negatives; Jiménez-Valverde & Lobo, 2007), with respect to a consensual map of beech observed presence in Europe, and amounted to 0.167 (SI Section S1). Assuming this fitness threshold constant under future climate, we used it in the demographic model to trigger tree mortality due to adverse climatic conditions.

Modelling migration and demography (Figure S2 in Section S2)

Model overview. The Gibbs-based migration model assumes that each species has an inherent spatial pattern, resulting from dispersal and post-dispersal processes such as intra or inter-specific interactions (competition) (Saltré *et al.*, 2009). The position of each tree and thereby the resulting spatial pattern is determined by the 'interaction potential function' (IPF), which describes local interactions between trees as a function of their pairwise geographic distance. This function therefore summarizes all dispersal and post-dispersal processes responsible for the spatial pattern of the forest. The IPF defines the probability that a tree be at a certain distance from another one. Positive IPF defines repulsion areas while negative IPF defines attraction areas. The IPF is parameterized using positions of tree in forest stand. The IPF can be defined for individual trees or for cohorts, here defined as groups of individuals of the same age in interaction with each other and experiencing the same local environmental conditions in a landscape. The principle of the model is that the inherent spatial pattern of the species is reproduced when the sum of all interactions (as defined by the IPF) is minimized using an iterative approach (SI Section S3). To couple the migration model with the habitat suitability model, we downscaled PHENOFIT's outputs from 10′ (i.e. the original climate resolution) to a 5 km resolution by a nearest neighbour interpolation method. Note

that the Gibbs-based migration model may be coupled with any type of SDM.

Demography. We assume that fitness, as calculated by PHENOFIT, is an accurate proxy for the carrying capacity (maximum number of cohorts). For each grid cell, a carrying capacity is calculated using a linear relationship to the grid-cell fitness. The maximum carrying capacity is fixed at five cohorts for computational constraints (for the maximum fitness index of 1). Cohorts older than 45 years are considered sexually mature (Ellenberg, 1988) throughout Europe whatever the climatic conditions. Different generation times do exist for beech (e.g. 60 years, Lischke & Löffler, 2006), especially towards range margins, but this is not taken into account here. The initial set of cohorts used for the starting of simulations is randomly aged between the age at maturation and the maximal age for beech (i.e. 45–300 years old). Pixels harbouring mature individuals periodically (every 3 years, periodicity based on beech massive seed production data from the French National Forests Office, ONF) produce a number of new offspring cohorts.

The number of offspring cohorts depends on the local suitability of climate for beech, i.e. it is proportional to the annual fitness predicted by PHENOFIT, so that no offspring are generated if fitness < fitness threshold and five new offsprings are generated if fitness = 1.

The model simulates both mortality linked to the age of each cohort and mortality driven by climatic constraints. Cohorts reaching 300 years or located in climatically unsuitable habitat (as inferred by PHENOFIT) are suppressed, to respectively reproduce age mortality and climatic constraints. If climate becomes unsuitable in a grid cell, cohorts are suppressed starting by the youngest cohort (randomly chosen in case of even-aged cohorts) until satisfying the grid cell's carrying capacity condition. Note that mortality driven by non-environmental factors mainly affects the initial set of cohorts randomly aged between 45 and 300 years old, because new offspring cannot reach the mortality age within the simulation's time range. This means the maximal lifetime is mainly driven by environmental conditions in the simulations.

Migration. The Gibbs-based migration model works in a continuous space (see details about simulation conditions in the SI Section S2). Offspring cohorts are first randomly placed within a radius of $\alpha = 9000$ m (chosen *a priori* and set up longer than the diagonal of a grid cell, 7071 m, so that an offspring cohort can fall into a surrounded grid cell whatever its parent location and the dispersal trajectory), which is one of the IPF parameters, from a randomly chosen mature parent cohort. They are then spatially arranged using a 'depletion-replacement' optimization process as a function of topographical constraints (see details in Saltré *et al.*, 2009 and SI Section S2), i.e. they are repositioned over the entire landscape until the sum of interactions calculated between every pair of cohorts is minimal, thus reproducing the empirical spatial pattern of the species. Minimization of the sum of interactions between cohorts, as described by the IPF, ensures that at the end of the process, their position in the landscape follows the

spatial pattern characteristic of the species. Offspring cohorts can establish if both the fitness of the final recipient grid cell and slope (derived from a digit elevation model) allow it, otherwise they are suppressed (see Demography section). Each grid cell presents a value of slope expressed as a probability of establishment for each cohort such as increasing slope decreased the probability of establishment (see detail SI Section S2). At each time step, the Gibbs-based migration model provides the position of tree cohorts in a continuous space, while the fitness simulated by PHENOFIT provides the maximal number of cohorts that can coexist in a grid cell of 5 km × 5 km (i.e. its carrying capacity). Because of computational constraints, a maximum of 5 cohorts were allowed to coexist on any given grid-cell.

Model calibration. The IPF was parameterized using the position of each tree of a beech forest stand in the Italian Alps (Figure S3a in Section S3). The calibration site is an unmanaged even-aged pure beech stand of 0.4 km², located in the northeastern Italian pre-Alps (46°02′N, 12°25′E) on the Cansiglio's Karst Plateau. However, this individual-based parameterization could not be used straightaway because (i) computational constraints limit the maximal number of tree simulated throughout Europe over the 21st century and (ii) tree interactions are captured until 200 m, which is a too short distance to account for some long-distance migration events. Therefore, the IPF function was parameterized on a simulated forest stand of 25 km². This simulated forest stand was obtained using a homogeneous Gibbs process (see Saltré *et al.*, 2013 for details) that successfully reproduces the spatial pattern of the smaller stand (Figure S4 in Section S3), i.e. using the individual-based IPF and assuming that local interactions (when considering individual trees) drive species spatial patterns at broader spatial scale (Pommerening & Stoyan, 2008). Such a simulated dataset allowed us to (i) define cohorts of high density of tree (≥0.81 tree per m²) which reduces the number of 'entities' to simulate by the model and (ii) parameterize a cohort-based IPF (Figure S3b in Section S3) able to capture cohort's interactions over 5 km, a sufficient distance to capture most of long-distance migration events (≈ 1 km^{-1}, Clark, 1998). The cohort's spatial scale corresponds to the highest spatial resolution we can use to simulate yearly individual-based migration throughout Europe because of computational constraint. This function was previously validated by simulating beech post-glacial colonization of Europe over the last 12 000 years (Saltré *et al.*, 2013).

The IPF parameters were fitted to the spatial pattern of the forest stand, as described by the pair correlation function $g(r)$ (Pommerening, 2002). Optimization was carried using a simulated annealing method (Kirkpatrick *et al.*, 1983) following an algorithm of Metropolis *et al.* (1953), with fit quality assessed using a least square criterion (see details in SI Section S3). Note that we assume null interactions between cohorts beyond 5000 m (i.e. size of a grid cell, see SI Section S3), but this does not exclude dispersal beyond this limit because spatial optimization promotes the establishment of cohorts having null or negative interactions (i.e. attraction effect compared to cohort having positive interactions (i.e. repulsion
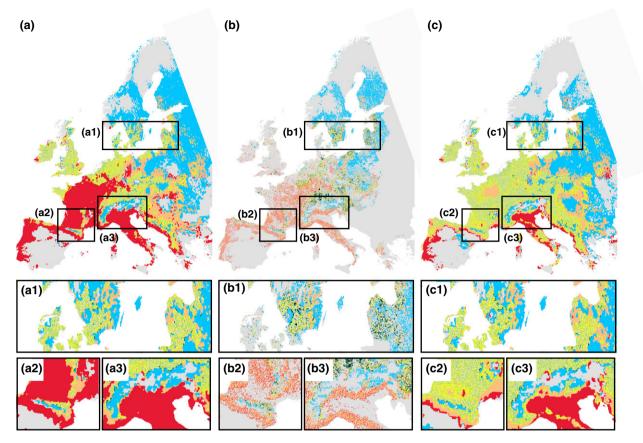
Fig. 1 Change in the distribution of *Fagus sylvatica*, when accounting for demography and migration, between 1981–2000 (20-years mean) and 2081–2100 (20-years mean) according to two greenhouse gas emission scenarios: a1Fi (a and b) and b2 (c), and the land use scenario GRAS (b). Grey: absence of the species; red: species range contraction due to climate unsuitability; orange: species present in 1981–2000 but extinct in 2081–2100 due to demographic collapse; yellow: population density decrease; green: population density increase; black: colonized suitable habitat; blue: uncolonized suitable habitat.

effect). Because the initial dataset was from a single, even-aged, pure stand, no data is available to assess (i) spatial or temporal variability in the IPF; (ii) age variability in the IPF, nor (iii) how interspecific competition affects the IPF. Thus, we assumed a unique IPF (see details on the IPF function used in SI Section S3 and Figure S3). For a detailed description of model-based parameter sensitivity, see Saltré *et al.* (2009).

Statistical analysis

Using a partial regression, we estimated the relative effect of four variables: (i) winter temperatures (more coupled with beech occurrence than summer temperatures, Fang & Lechowicz, 2006); (ii) annual precipitations; (iii) demography/migration (accounting for both migration and demography processes) and (iv) land use. The adjusted R^2 significance was tested with F-statistic using a permutation of the residuals due to their non-normality (Legendre & Legendre, 1998). To account for spatial autocorrelation, we also compared the likelihoods of all 32 Generalized Least Squares models corresponding to all combinations of all explanatory variables

affecting the rates of expansion or contraction, assuming a Gaussian spatial autocorrelation structure. We evaluated the AIC of each model, and for each of the five tested variables, computed the Akaike weights of all models assuming this variable affected the rate of expansion or contraction. From these weights, we derived the evidence ratios supporting (or not) the contribution of each variable to explaining variation in these rates (Massol *et al.*, 2007).

Results

European beech range shifts under future climate scenarios

Results show expansion of beech's climatically suitable habitats by 2100 towards north-eastern Europe and upward in altitude, especially in the Alps and the Pyrenees (blue and black pixels in Fig. 1a), and a strong decrease in suitable areas in Western Europe, especially under scenario A1Fi (red and orange in Fig. 1a). The
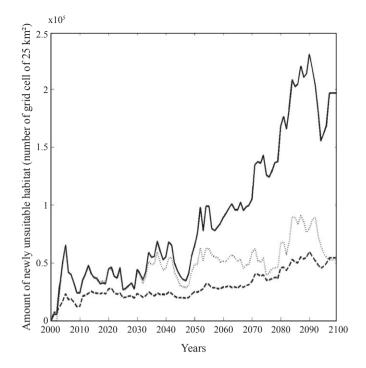
Fig. 2 Forecast new unsuitable areas throughout the 21st century. The graph shows the amount of new climatically unsuitable 5 km² grid-cells through time (as compared with 1981–2000, 20-years mean). The black line displays results under A1Fi, the dotted line results under A1Fi-GRAS and the dashed line under B2 scenario.

area of climatically unsuitable habitats increases over time whatever the climate scenario; however, much less under scenario B2, with strong increases under scenario A1Fi around years 2005, 2040, 2055, 2075 and 2090, indicating particularly climatically unsuitable years for beech (Fig. 2).

Future climate conditions are projected as suitable for beech in a wider region in north-eastern Europe under both scenarios: the future beech potential range size represents 125% and 141% of its current potential range size under A1Fi and B2 respectively, i.e. a gain of 0.9 million km² and 1.5 million km² respectively (Tables 1 and 2; Fig. 1 black and blue regions). However, only a small proportion of the newly suitable area (1% under scenario A1Fi and 2% under scenario B2) is effectively colonized when migration and demography are accounted for (Tables 1 and 2), and the main differences between the two scenarios take place in the Alps and in northern Europe (black areas on Fig. 1).

Conversely, taking demography and migration into account unexpectedly increases the contraction area (by 163% under scenario A1Fi and by 370% under B2, Tables 1 and 2). Areas where beech populations are going extinct due to demographic collapse (i.e. simulated fitness drops below the critical threshold of 0.167 at a frequency that does not allow offspring cohorts to reproduce) rather than unsuitable climate conditions (i.e. the simulated fitness is constantly below the critical threshold of 0.167) are mainly located in France and in Eastern Europe (orange areas in Fig 1a and c).

Table 1 Size of simulated potential and realized areas (×10³ km²) under current (1981–2000) and future conditions (2081–2100, A1Fi, A1Fi-Gras, and B2). Colonized and lost areas respectively represent newly suitable and newly unsuitable habitats in 2081–2100 (respectively blue/black and red/orange areas in Fig. 1)

	Total area (×10³ km²)		Colonized area (×10³ km²)		Lost area (×10³ km²)	
	Potential	Realised	Potential	Realised	Potential	Realised
Current	3623	3541				
A1Fi	4530	1392	2245	31	1337	2180
A1Fi-Gras	1342	324	886	68	373	565
B2	5100	2260	1821	34	360	1332

Table 2 Filling rate of the potential distribution and range size change between 1981–2000 and 2081–2100. Realised/Potential: ratio of the realized distribution area to that of the potential distribution in 2081–2100 (20-years mean) calculated for (i) the entire distribution; (ii) only for colonized areas and (iii) only for the contracted areas. Range size change is calculated assuming unlimited migration (potential distribution) and realistic migration (realized distribution), as the difference between the beech range size in 2081–2100 (20-years mean) and its range size in 1981–2000 (20-years mean)

	Range size change (%)		Realised/Potential (%)		
	Potential	Realised	Total area	Colonized area	Lost area
A1Fi (compared to 1981–2000	125	39	31	1	163
A1Fi-Gras (compared to A1Fi)	30	23	24	8	151
B2 (compared to 1981–2000)	141	64	44	2	370

Land use drastically reduces beech range size by 30% in 2100 (i.e. a loss of 3.2×10^6 km² Tables 1 and 2). Land use change increases the proportion of suitable habitats effectively colonized (8% of the suitable areas vs. 1%, which represents a net gain of about 37×10^3 km²); and it decreases the proportion of effectively contracted areas (151% vs. 163%, which represents a net gain of about 1615×10^3 km²) (Tables 1 and 2).

Climate variables and ecological processes affecting beech distribution

New suitable habitats in 2081–2100 tend to be wetter than in 1981–2000 (+5 mm yr^{-1} and +2.5 mm yr^{-1} in annual precipitations under scenarios A1Fi and B2 respectively, white boxes in Fig. 3b), while new unsuitable habitats tend to be significantly drier (9 mm yr^{-1} and −4 mm yr^{-1} in annual precipitations under scenarios A1Fi and B2 respectively, grey boxes in Fig. 3b). Both suitable and unsuitable new areas are forecast to be significantly warmer than observed in 1981–2000 (Fig. 3a), including during winter (+6.1 °C vs. +5.2 °C and +3.2 °C vs. +3.1 °C in coldest month temperature under A1Fi and B2 respectively, Fig. 3c), which increases drought stress.

PHENOFIT outputs indicate that fitness is limited by drought both under current (32% of 1980–2000 unsuitable habitat, Fig. 4) and future scenarios (34% of unsuitable
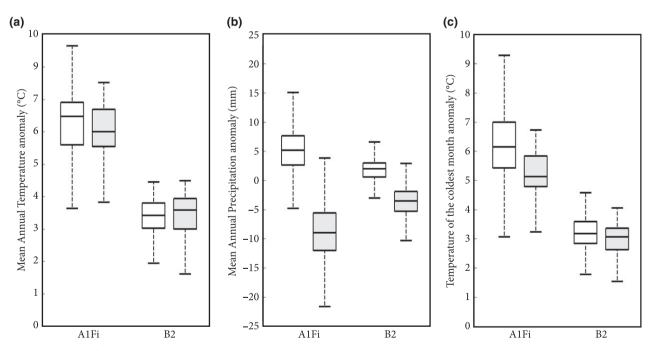

Fig. 3 Boxplots of anomalies of mean annual temperature (a), mean annual precipitation (b) and mean temperature of the coldest month (c) under two climate scenarios (A1Fi and B2) in 2081–2100 with respect to 1981–2000 (20-years mean). White boxplots correspond to newly suitable areas (blue and black areas in Fig. 1) and grey boxplots correspond to newly unsuitable areas (red and orange areas in Fig. 1). For each boxplot, the central mark is the median, the edges of the box are the 25th and 75th percentiles, and the whiskers extend to the extreme data points not considered as outliers.
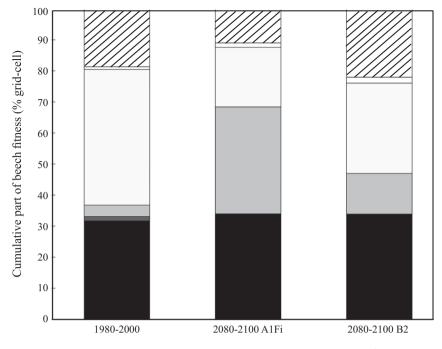
Fig. 4 Biological processes limiting fitness. The plot shows the fraction of climatically unsuitable 10′ pixels in which beech fitness is primarily limited by drought, killing frost, failure of bud dormancy break, frozen leaves, frozen flowers (grey scale from black to white) and low fruit maturation success (diagonal hatching), in 1981–2000 and 2081–2100 under A1Fi and B2 scenarios.

habitat under both A1Fi and B2). However, future climatically unsuitable areas are mainly characterized by limitations due to chilling requirement to break bud dormancy under A1Fi (34% of unsuitable habitat) and leaf frost resistance (29% of unsuitable habitat) under scenario B2. Failure of dormancy break is projected to occur mainly in western and central Europe under A1Fi, lethal drought is projected to occur in many areas of southern Europe under both scenarios (Figure S6 in Section S7).

Beech migration rates under future scenarios

The variation partitioning analysis of beech expansion and contraction rates shows that the temperature of the coldest month and land use change explained the greatest amount of variation in expansion rate (respectively 8.9% and 4.1%, with $P < 0.05$ for each of them, SI Table S1 in Section S5), whereas annual precipitation and the migration/demography variable explained the greatest amount of variation in range contraction (respectively 8.6%, and 5.3% with $P < 0.05$ for each of them). These are supported by the evidence ratios (Massol *et al.*, 2007) of all variables (>5.6) indicating that all variables contribute significantly to explaining variation in both rates, even when the number of degrees of freedom is deflated due to non-independence among pixels.

The expansion rate of beech realized distribution is much slower than that of its potential distribution (med-

ian rate of 44 m yr^{-1} vs. 207 m yr^{-1} and 22 m yr^{-1} vs. 152 m yr^{-1} under A1Fi and B2 respectively, Fig. 5a; Table S2 in Section S6). Conversely and unexpectedly, the contraction rate of beech realized distribution is much faster than that of its potential distribution (median rate of 333 m yr^{-1} vs. 284 m yr^{-1} and 154 m yr^{-1} vs. 109 m yr^{-1} under A1Fi and B2 respectively Fig. 5a; Table S2 in Section S6). Accounting for land use slows down both the expansion and contraction rates of the potential distribution (median rates: 138 m yr^{-1} vs. 207 m yr^{-1} and 127 m yr^{-1} vs. 284 m yr^{-1} respectively). However, while accounting for land use decreased the expansion of the realized distribution (22 m yr^{-1} vs. 44 m yr^{-1}), it had only a minor influence on the contraction rate (328 m yr^{-1} vs. 333 m yr^{-1}).

Mean expansion rates of the potential and the realized distributions both decrease throughout the 21st century with a sharp decline from 2000 to 2040 (Fig. 5b). Beyond 2050, the two climate scenarios A1Fi and B2 diverge: expansion and contraction rates decrease under B2 while they slightly increase under A1Fi (green vs. red curves on Fig. 5b).

Discussion

Predicting species distribution change at a continental scale while accounting for demographic and migration processes has been a challenge for the
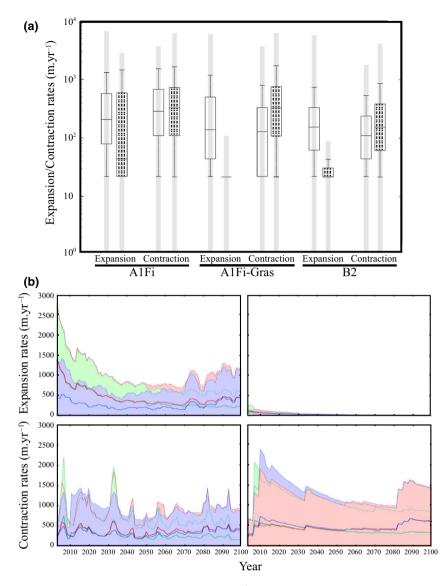
Fig. 5 (a) Boxplots of beech expansion and contraction rate (in m yr^{-1}) between 1981–2000 and 2081–2100 (20-years mean) assuming unlimited (white) and realistic (dashed) migration under A1Fi and B2 climate scenarios and GRAS land use scenario. For each boxplot, the central mark is the median, the edges of the box are the 25th and 75th percentiles, and the whiskers extend to the extreme data points not considered as outliers. Extreme events are given by both minimal and maximal values (shading). Spread rates are calculated from Euclidean distance between future and current beech distribution limits. Note the logarithmic scale for expansion/contraction rates. (b) Mean (bold curves) and standard deviation (envelopes and thin curves) of beech spread rate (m yr^{-1}, 5-years running mean) at the leading edge (upper panels) and at the trailing edge (lower panels) assuming unlimited migration (left panels) and realistic migration (right panels). Spread rate is calculated with Euclidean distance between future (every 5 years) and current beech distribution limits under A1Fi (red line and envelope) and B2 (green line and envelope) future climate scenarios and GRAS (blue line and envelope) future land use scenario.

ecological modelling community for many years. Here, we predict the potential and realized distribution changes of European beech throughout the 21st century, using a process-based SDM that accounts for important demographic and migration dynamics. The model was previously shown to have good prediction skill based on hindcasts over millennia

(Saltré et al., 2013). Our simulations highlight that even if new climatically suitable areas become available in the future, the interplay between future climate variability, land use change, limited migration ability, and slow life-history traits will likely prevent European beech from tracking its future optimal climate.

Ecological limits to beech potential distribution

PHENOFIT incorporates the well-known sensitivity of beech to drought (Geßler *et al.*, 2007; Mátyás *et al.*, 2010) and frost (Dittmar & Elling, 2006; Kreyling *et al.*, 2012) as well as its chilling requirement in winter to achieve bud dormancy release (Heide, 1993).

The model predicts a shift of beech climatically suitable habitats towards north-eastern Europe and up mountains such as the Alps, Pyrenees and Carpathians (Fig. 1). These results are in agreement with previous modelling studies (Sykes & Prentice, 1996; Koca *et al.*, 2006; Rickebusch *et al.*, 2008; Kramer *et al.*, 2010; Meier *et al.*, 2012). Newly suitable habitats are the result of forecasted warmer and wetter conditions by the end of the 21st century, while newly unsuitable habitats are the result of warmer and drier forecasted conditions (Fig. 3).

At the leading edge (North-eastern Europe), both cold temperatures and drought currently limit beech distribution (Bolte *et al.*, 2007; Packham *et al.*, 2012). However, both of these limiting factors are projected to decrease in the future in North-Eastern Europe, with winters maintaining cold enough temperatures for bud dormancy to be broken (Figure S6 in Section S7). Warmer temperatures, especially in spring and summer, increase the probability of fruit maturation success, also enhanced by reduced frost damages to leaves (Fig. 4a, and Figure S6 in Section S7).

At the trailing edge of the distribution, projected beech range contraction is caused both by warmer winters, preventing bud dormancy break (especially under scenario A1Fi, Fig. 4a, Figure S6 in Section S7) and subsequent leaf unfolding and flowering, and by increases in drought (Figure S6 in Section S7). These results are well supported by recent observations suggesting that temperature rises and associated decreases in precipitation (mainly the effect of lower amount of annual precipitation on the precipitation seasonality) has increased drought stress for beech and is responsible for population decline at the trailing edge of its distribution (Jump *et al.*, 2006; Allen *et al.*, 2010; Mátyás *et al.*, 2010).

Climate variability, slow life-history, and migration dramatically reduce the velocity of beech range shift

Although climate has long been emphasized as the main control of species distributions at global scales (Pearson & Dawson, 2003), recent studies suggest that the role of migration has probably been underestimated (Svenning & Skov, 2004, 2007; Fang & Lechowicz, 2006; Svenning *et al.*, 2008). Under rapidly changing climates, migration limitation is expected to

have an even greater impact on species range shifts (Zhu *et al.*, 2012). This is particularly true of late-successional species such as beech, whose dispersal abilities are lower than those of pioneer species such as birch (Meier *et al.*, 2011).

Our simulations show that migration limitation will strongly affect the future range dynamics of beech, preventing the species from colonizing newly suitable habitats (Fig. 1), so that in 2100 beech distribution is projected to be strongly in disequilibrium with climate. Migration limitation leads to a drastic contraction of beech distribution by 2100 (the modelled future beech realized range size represents 39% or 64% of its modelled current realized range size under A1Fi and B2 respectively, Table 2), although suitable habitats are substantially enlarged (the future beech potential range size represents 125% in scenario A1Fi and 141% in scenario B2 of its current potential range size).

Although the forecasted velocity of change in suitable habitats at the end of the 21st century (median velocity 1500 m yr^{-1}, Fig. 5b) is twice that of the maximal velocity achieved in simulations over the past 12 000 years (median velocity of suitable habitats 700 m yr^{-1}; Fig. 4a in Saltré *et al.*, 2013), the expansion rates of the realized distribution at the end of the 21st century are much lower than that simulated over the past 12,000 years (median expansion rate of 20 m yr^{-1} for the 21st century, Fig. 5a, vs. 280 m yr^{-1} over the Holocene, Saltré *et al.*, 2013). Although these lower mean expansion rates might be partly due to higher competition in the future than during the Holocene (Feurdean *et al.*, 2013), we argue that demographic collapses after 2050, due to a higher climate variability in both A1Fi and B2 scenarios than during the Holocene climate (Figure S7 in Section S8; Salinger, 2005) with especially more intense drought like conditions (Rasztovits *et al.*, 2014; Thiel *et al.*, 2014), caused sudden extensive mortality. The fast switching (a few years) between unsuitable and sub-optimal climate conditions prevents neighbouring populations from recolonizing these areas (orange pixels in Fig. 1). Accounting for demography/migration in our simulations slowed down expansion rates of the northern beech population, while at the same time unexpectedly accelerating contraction rates of southern beech populations (Table S2 in Section S6). As a result of these demographic processes, future migration rates are characterized by a larger variation in migration rates than during the Holocene, with both shorter and longer distance events (i.e. <40 m yr^{-1} and >2500 m yr^{-1} under A1Fi, Fig. 5a) than under the last millennia (Fig. 4b in Saltré *et al.*, 2013). This result emphasizes the importance of taking both dispersal and demographical processes into

account in a climate change context to better understand range dynamics (Dullinger *et al.*, 2012; Pagel & Schurr, 2012; Schurr *et al.*, 2012; Fordham *et al.*, 2013b).

Land use impacts on beech range shift

Our simulations suggest that European beech will not be able to track its future optimal climate because its expansion and contraction rates are strongly constrained by the projected climate variability, limited migration, and landscape fragmentation. A similar conclusion was made for Australian plants (Fordham *et al.*, 2012). Land use and rising temperatures are expected to affect the expansion rate of beech at the leading edge. Towards its trailing edge, drought stress and elevated winter temperatures, together with the slow demography of beech and its limited migration ability (preventing recolonization in unstable climate conditions – orange pixels in Fig. 1) are expected to affect its contraction rate (Table S1 in Section S5).

In agreement with Meier *et al.* (2012), we found that human-driven land use strongly affected both the shape and the size of the projected distribution of beech. Accounting for land use in our simulations reduces the size of the potential distribution of beech by 70% under the A1Fi scenario (Table 2), slightly increasing the proportion of suitable habitats that could be colonized (8% vs. 1% without taking land use into account, Table 2), and slightly decreasing the ratio of effectively to potentially lost area (151% vs. 163% without accounting for land use). The GRAS land use scenario projects land abandonment and forest planting in Eastern Europe, within the core of the distribution of European beech (Figure S8 in Section S9). This land abandonment generates many accessible suitable patches, where local colonization/extinction dynamics ensure a high local expansion rate (Fig. 5b). On the contrary, towards the leading edge, habitat fragmentation slows down the simulated expansion of beech (Pitelka *et al.*, 1997; Meier *et al.*, 2011; Feurdean *et al.*, 2013; Fig. 5a and b), and rare long-distance events are the main way to reach patches of suitable habitats (Table S2 in Section S6; Clark, 1998; Nathan *et al.*, 2008).

Limits to our study and directions for future research

Accounting for migration and demography yields much more pessimistic projections of beech distribution than suggested by changes in climatically suitable areas (Table 1, Fig. 1). This is because the interplay of demographic and migration processes reduces the range expansion rate while increasing the contraction rate. Nevertheless, adaptive responses of migration or phenology could increase the expansion rate of beech

at the leading edge of its distribution, and/or decrease its contraction rate at the trailing edge (Kramer *et al.*, 2010). Rapid evolution of such traits under strong selective pressures induced by climate warming has been documented in a large number of organisms in the last decade (e.g. Thomas *et al.*, 2001; Berteaux *et al.*, 2004; Kovach *et al.*, 2012). Indeed, phenological traits show intra- and interpopulation variation that can fuel micro-evolution even in long generation time organisms such as trees (Mimura & Aitken, 2010).

Although the Gibbs-based migration model takes intra-specific competition into account, interspecific interactions (such as competition) were neglected. The main competitors of beech, i.e. *Picea abies*, *Abies alba* and *Quercus sp.*, were not considered in this study and they could be an important determinant of its distribution preventing its establishment (Bjorkman & Bradshaw, 1996), modifying its migration pathways (Watson, 1996) and decreasing its migration rate (Meier *et al.*, 2011). Nevertheless, we argue that inter-specific competition can be neglected, as a first approximation, when we look at demography during expansion for two main reasons. First, at the northern range margins, projected rising temperatures would lead to more mesic climatic conditions, making beech a stronger competitor, decreasing the effect of biotic interactions (Pelachs *et al.*, 2009). Second, results of Meier *et al.* (2011), which have taken interspecific competition into account in their simulations using different kinds of models, support our simulation outputs, and therefore suggest that interspecific competition has not a strong effect on beech future migration rate. Note, however, that the Gibbs-based migration model can be parameterized to handle mixed forests, accounting for interspecific competition using marked Gibbs point processes (Stoyan & Stoyan, 1998).

Other limitations to our study are that we calibrated the migration model using data from a single beech stand, thus assuming (i) that the information from one forest stand can be used to interpret spatial processes at the scale of Europe; (ii) and that landscape fragmentation did not influence the behaviour of the dispersal agent (Nathan *et al.*, 2002). We also neglected human-assisted migration, a potential source of long-distance dispersal event (Feurdean *et al.*, 2013). Finally, we assumed a constant fitness threshold in the future (to transform fitness into species presence and absence) that might impact the projected distribution and therefore the projected colonization and extinction rates (Nenzen & Araújo, 2011).

Nevertheless, we argue that these shortcomings should have minor impact on our projections because (i) IPF successfully reproduces a spatial pattern

observed in others beech forest throughout Europe (Figure S4 in Section S3); (ii) the migration model simulates realistic age distribution across the range (Figure S5 in Section S4); and (iii) the migration model reproduced beech post-glacial colonization rates and routes successfully over 12 000 years (Saltré *et al.*, 2013).

References

Allen CD, Macalady AK, Chenchouni H *et al.* (2010) A global overview of drought and heat-induced tree mortality reveals emerging climate change risks for forests. *Forest Ecology and Management*, **259**, 660–684.

Barve N, Barve V, Jimenez-Valverde A *et al.* (2011) The crucial role of the accessible area in ecological niche modeling and species distribution modeling. *Ecological Modelling*, **222**, 1810–1819.

Beale CM, Lennon JJ (2012) Incorporating uncertainty in predictive species distribution modelling. *Philosophical Transactions of the Royal Society B: Biological Sciences*, **367**, 247–258.

Berteaux D, Réale D, McAdam AG, Boutin S (2004) Keeping pace with fast climate change: can artic life count on evolution? *Integrative and Comparative Biology*, **44**, 140–151.

Bjorkman L, Bradshaw R (1996) The immigration of *Fagus sylvatica L* and *Picea abies (L) Karst* into a natural forest stand in southern Sweden during the last 2000 years. *Journal of Biogeography*, **23**, 235–244.

Bolte A, Czajkowski T, Kompa T (2007) The north-eastern distribution range of European beech – a review. *Forestry*, **80**, 413–429.

Chuine I (2010) Why does phenology drive species distribution? *Philosophical Transactions of The Royal Society B: Biological Sciences*, **365**, 3149–3160.

Chuine I, Beaubien EG (2001) Phenology is a major determinant of tree species range. *Ecology Letters*, **4**, 500–510.

Clark JS (1998) Why trees migrate so fast: confronting theory with dispersal biology and the paleorecord. *American Naturalist*, **152**, 537–554.

Cleland EE, Chuine I, Menzel A, Mooney HA, Schwartz MD (2007) Shifting plant phenology in response to global change. *Trends in Ecology & Evolution*, **22**, 357–365.

Cleland EE, Allen JM, Crimmins TM *et al.* (2012) Phenological tracking enables positive species responses to climate change. *Ecology*, **93**, 1765–1771.

Collingham YC, Huntley B (2000) Impacts of habitat fragmentation and patch size upon migration rates. *Ecological Applications*, **10**, 131–144.

Delpierre N, Dufrêne E, Soudani K, Ulrich E, Cecchini S, Boé J, François C (2009) Modelling interannual and spatial variability of leaf senescence for three deciduous tree species in France. *Agricultural and Forest Meteorology*, **149**, 938–948.

Dittmar C, Elling W (2006) Phenological phases of common beech (Fagus sylvatica L.) and their dependence on region and altitude in Southern Germany. *European Journal of Forest Research*, **125**, 181–188.

Dormann CF, Schymanski SJ, Cabral J *et al.* (2012) Correlation and process in species distribution models: bridging a dichotomy. *Journal of Biogeography*, **39**, 2119–2131.

Dullinger S, Gattringer A, Thuiller W *et al.* (2012) Extinction debt of high-mountain plants under twenty-first-century climate change. *Nature Climate Change*, **2**, 619–622.

Ellenberg H (1988) *Vegetation Ecology of Central Europe*. Cambridge University Press, Cambridge.

Fang J, Lechowicz MJ (2006) Climatic limits for the present distribution of beech (*Fagus L.*) species in the world. *Journal of Biogeography*, **33**, 1804–1819.

Feurdean A, Bhagwat SA, Willis KJ, Birks HJB, Lischke H, Hickler T (2013) Tree migration-rates: narrowing the gap between inferred post-glacial rates and projected rates. *PLoS ONE*, **8**, e71797.

Fordham DA, Akcakaya HR, Araújo MB *et al.* (2012) Plant extinction risk under climate change: are forecast range shifts alone a good indicator of species vulnerability to global warming? *Global Change Biology*, **18**, 1357–1371.

Fordham DA, Akçakaya HR, Araújo MB, Keith DA, Brook BW (2013a) Tools for integrating range change, extinction risk and climate change information into conservation management. *Ecography*, **36**, 956–964.

Fordham DA, Akcakaya R, Brook BW *et al.* (2013b) Adapted conservation measures are required to save the Iberian lynx in a changing climate. *Nature Climate Change*, **3**, 899–903.

Fordham DA, Mellin C, Russell BD *et al.* (2013c) Population dynamics can be more important than physiological limits for determining range shifts under climate change. *Global Change Biology*, **19**, 3224–3237.

Geßler A, Keitel C, Kreuzwieser J, Matyssek R, Seiler W, Rennenberg H (2007) Potential risks for European beech (*Fagus sylvatica L.*) in a changing climate. *Trees*, **21**, 1–11.

Gordon C, Cooper C, Senior CA *et al.* (2000) The simulation of SST, sea ice extents and ocean heat transports in a version of the Hadley Centre coupled model without flux adjustments. *Climate Dynamics*, **16**, 147–168.

Gritti ES, Duputié A, Massol F, Chuine I (2013) Estimating consensus and associated uncertainty between inherently different species distribution models. *Methods in Ecology and Evolution*, **4**, 442–452.

Guisan A, Zimmermann NE (2000) Predictive habitat distribution models in ecology. *Ecological Modelling*, **135**, 147–186.

Heide OM (1993) Dormancy release in beech buds (Fagus sylvatica) requires both chilling and long days. *Physiologia Plantarum*, **89**, 187–191.

Holt RD, Lawton JH, Gaston KJ, Blackburn TM (1997) On the relationship between range size and local abundance: back to basics. *Oikos*, **78**, 183–190.

Jiménez-Valverde A, Lobo JM (2007) Threshold criteria for conversion of probability of species presence to either-or presence-absence. *Acta Oecologica*, **31**, 361–369.

Jump AS, Hunt JM, Penuelas J (2006) Rapid climate change-related growth decline at the southern range edge of Fagus sylvatica. *Global Change Biology*, **12**, 2163–2174.

Kearney M, Porter W (2009) Mechanistic niche modelling: combining physiological and spatial data to predict species' ranges. *Ecology Letters*, **12**, 334–350.

Kirkpatrick S, Gelatt CD, Vecchi MP (1983) Optimization by simulated annealing. *Science*, **220**, 671–680.

Koca D, Smith B, Sykes MT (2006) Modelling regional climate change effects on potential natural ecosystems in Sweden. *Climatic Change*, **78**, 381–406.

Kovach RP, Gharrett AJ, Tallmon DA (2012) Genetic change for earlier migration timing in a pink salmon population. *Proceedings of the Royal Society B-Biological Sciences*, **279**, 3870–3878.

Kramer K, Degen B, Buschbom J, Hickler T, Thuiller W, Sykes MT, de Winter W (2010) Modelling exploration of the future of European beech (*Fagus sylvatica L.*) under climate change – Range, abundance, genetic diversity and adaptive response. *Forest Ecology and Management*, **259**, 2213–2222.

Kremer A, Ronce O, Robledo-Arnuncio JJ *et al.* (2012) Long-distance gene flow and adaptation of forest trees to rapid climate change. *Ecology Letters*, **15**, 378–392.

Kreyling J, Thiel D, Nagy L, Jentsch A, Huber G, Konnert M, Beierkuhnlein C (2012) Late frost sensitivity of juvenile *Fagus sylvatica L.* differs between southern Germany and Bulgaria and depends on preceding air temperature. *European Journal of Forest Research*, **131**, 717–725.

Legendre P, Legendre L (1998) *Numerical Ecology*. Elsevier Science, Amsterdam.

Lischke H, Löffler TJ (2006) Intra-specific density dependence is required to maintain species diversity in spatio-temporal forest simulations with reproduction. *Ecological Modelling*, **198**, 341–361.

Malanson GP, Armstrong MP (1996) Dispersal probability and forest diversity in a fragmented landscape. *Ecological Modelling*, **87**, 91–102.

Massol F, David P, Gerdeaux D, Jarne P (2007) The influence of trophic status and large-scale climatic change on the structure of fish communities in Perialpine lakes. *Journal of Animal Ecology*, **76**, 538–551.

Mátyás C, Berki I, Czucz B, Gálos B, Moricz N, Rasztovits E (2010) Future of beech in southeast Europe from the perspective of evolutionary ecology. *Acta Silvatica et Lignaria Hungarica*, **6**, 91–110.

Meier ES, Edwards TC, Kienast F, Dobbertin M, Zimmermann NE (2011) Co-occurrence patterns of trees along macro-climatic gradients and their potential influence on the present and future distribution of Fagus sylvatica L. *Journal of Biogeography*, **38**, 371–382.

Meier ES, Lischke H, Schmatz DR, Zimmermann NE (2012) Climate, competition and connectivity affect future migration and ranges of European trees. *Global Ecology & Biogeography*, **21**, 164–178.

Metropolis N, Rosenbluth AW, Rosenbluth MN, Teller AH, Teller E (1953) Equation of state calculation by fast computing machines. *Journal of Chemical Physics*, **21**, 1087–1092.

Mimura M, Aitken SN (2010) Local adaptation at the range peripheries of Sitka spruce. *Journal of Evolutionary Biology*, **23**, 249–258.

Mitchell CD, Jones PD (2005) An improved method of constructing a database of monthly climate observations and associated high-resolution grids. *International Journal of Climatology*, **25**, 693–712.

Mitchell TD, Carter TR, Jones PD, Hume M, New M (2004) A comprehensive set of high-resolution grids of monthly climate for Europe and the globe: the observed record (1901–2000) and 16 scenarios (200–2100). *Tyndall Center Working Paper*, **55**, 30.

Morin X, Chuine I (2005) Sensitivity analysis of the tree distribution model PHENO-FIT to climatic input characteristics: implications for climate impact assessment. *Global Change Biology*, **11**, 1493–1503.

Morin X, Augspurger C, Chuine I (2007) Process-based modeling of tree species' distributions: what limits temperate tree species' range boundaries? *Ecology*, **88**, 2280–2291.

Morin X, Viner D, Chuine I (2008) Tree species range shifts at a continental scale: new predictive insights from a process-based model. *Journal of Ecology*, **96**, 784–794.

Morin X, Lechowicz MJ, Augspurger C, O'Keefe J, Viner D, Chuine I (2009) Leaf phenology changes in 22 North American tree species during the 21st century. *Global Change Biology*, **15**, 961–997.

Nathan R, Katul GG, Horn HS *et al.* (2002) Mechanisms of long-distance dispersal of seeds by wind. *Nature*, **418**, 409–413.

Nathan R, Schurr FM, Spiegel O, Steinitz O, Trakhtenbrot A, Tsoar A (2008) Mechanisms of long-distance seed dispersal. *Trends in Ecology & Evolution*, **23**, 638–647.

Nenzen HK, Araújo MB (2011) Choice of threshold alters projections of species range shifts under climate change. *Ecological Modelling*, **222**, 3346–3354.

Nicks AD, Lane LJ, Gander GA (1995) Weather generator. In: *USDA-Water Erosion Prediction Project: Hillslope Profile and Watershed Model Documentation* (eds Flanagan DC, Nearing MA), pp. 1–22. NSERL, West Lafayette.

Normand S, Ricklefs RE, Skov F, Bladt J, Tackenberg O, Svenning JC (2011) Postglacial migration supplements climate in determining plant species ranges in Europe. *Proceedings of the Royal Society B-Biological Sciences*, **278**, 3644–3653.

Packham JR, Thomas PA, Atkinson MD, Degen T (2012) Biological flora of the British Isles: Fagus sylvatica. *Journal of Ecology*, **100**, 1557–1608.

Pagel J, Schurr FM (2012) Forecasting species ranges by statistical estimation of ecological niches and spatial population dynamics. *Global Ecology and Biogeography*, **21**, 293–304.

Pearson RG, Dawson TP (2003) Predicting the impacts of climate change on the distribution of species: are bioclimate envelope models useful? *Global Ecology and Biogeography*, **12**, 361–371.

Pelachs A, Perez-Obiol R, Ninyerola M, Nadal J (2009) Landscape dynamics of Abies and Fagus in the southern Pyrenees during the last 2200 years as a result of anthropogenic impacts. *Review of Palaeobotany and Palynology*, **156**, 337–349.

Pereira HM, Leadley PW, Proenca V *et al.* (2010) Scenarios for global biodiversity in the 21st century. *Science*, **330**, 1496–1501.

Peterson AT, Soberón J, Pearson RG, Anderson RP, Martínez-Meyer E, Nakamura M, Araújo MB (2011) *Ecological Niches and Geographic Distributions*. Princeton University Press, Princeton, New Jersey.

Pitelka LF, Gardner RH, Ash J *et al.* (1997) Plant migration and climate change. *American Scientist*, **85**, 464–474.

Pommerening A (2002) Approaches to quantifying forest structures. *Forestry*, **75**, 305–324.

Pommerening A, Stoyan D (2008) Reconstructing spatial tree point patterns from nearest neighbour summary statistics measured in small subwindows. *Canadian Journal of Forest Research-Revue Canadienne De Recherche Forestiere*, **38**, 1110–1122.

Pounds JA, Fogden MPL, Campbell JH (1999) Biological response to climate change on a tropical mountain. *Nature*, **398**, 611–615.

Pulliam HR (2000) On the relationship between niche and distribution. *Ecology Letters*, **3**, 349–361.

Rasztovits E, Berki I, Matyas C, Czimber K, Potzelsberger E, Moricz N (2014) The incorporation of extreme drought events improves models for beech persistence at its distribution limit. *Annals of Forest Science*, **71**, 201–210.

Rickebusch S, Thuiller W, Hickler T, Araújo MB, Sykes MT, Schweiger O, Lafourcade B (2008) Incorporating the effects of changes in vegetation functioning and CO2 on water availability in plant habitat models. *Biology Letters*, **4**, 556–559.

Rogelj J, Meinshausen M, Knutti R (2012) Global warming under old and new scenarios using IPCC climate sensitivity range estimates. *Nature Climate Change*, **2**, 248–253.

Sala OE, Chapin FS III, Armesto JJ *et al.* (2000) Global biodiversity scenarios for the year 2100. *Science*, **287**, 1770–1774.

Salinger MJ (2005) Climate variability and change: past, present and future – an overview. *Climatic Change*, **70**, 9–29.

Saltré F, Chuine I, Brewer S, Gaucherel C (2009) A phenomenological model without dispersal kernel to model species migration. *Ecological Modelling*, **220**, 3546–3554.

Saltré F, St-Amant R, Gritti ES, Brewer S, Gaucherel C, Davis BAS, Chuine I (2013) Climate or migration: what limited European beech post-glacial colonization? *Global Ecology & Biogeography*, **22**, 1217–1227.

Schurr FM, Pagel J, Cabral JS *et al.* (2012) How to understand species' niches and range dynamics: a demographic research agenda for biogeography. *Journal of Biogeography*, **39**, 2146–2162.

Snell RS, Huth A, Nabel JEMS *et al.* (2014) Using dynamic vegetation models to simulate plant range shifts. *Ecography*, doi: 10.1111/ecog.00580/abstract.

Stoyan D, Stoyan H (1998) Non-homogeneous Gibbs process models for forestry – a case study. *Biometrical Journal*, **40**, 521–531.

Svenning JC, Skov F (2004) Limited filling of the potential range in European tree species. *Ecology Letters*, **7**, 565–573.

Svenning JC, Skov F (2007) Could the tree diversity pattern in Europe be generated by postglacial dispersal limitation? *Ecology Letters*, **10**, 453–460.

Svenning J-C, Normand S, Skov F (2008) Postglacial dispersal limitation of widespread forest plant species in nemoral Europe. *Ecography*, **31**, 316–326.

Sykes MT, Prentice IC (1996) Climate change, tree species distributions and forest dynamics: a case study in the mixed conifer/northern hardwoods zone of northern Europe. *Climatic Change*, **34**, 161–177.

Thiel D, Kreyling J, Backhaus S *et al.* (2014) Different reactions of central and marginal provenances of Fagus sylvatica to experimental drought. *European Journal of Forest Research*, **133**, 247–260.

Thomas CD, Bodsworth EJ, Wilson RJ, Simmons AD, Davies ZG, Musche M, Conradt L (2001) Ecological and evolutionary processes at expending range margins. *Nature*, **411**, 577–581.

Thomas CD, Cameron A, Green RE *et al.* (2004) Extinction risk from climate change. *Nature*, **427**, 145–148.

Thuiller W, Lavorel S, Araùjo MB, Sykes MT, Prentice IC (2005) Climate change threats to plant diversity in Europe. *Proceedings of the National Academy of Sciences of the United States of America*, **102**, 8245–8250.

Walther GR, Post E, Convey P *et al.* (2002) Ecological responses to recent climate change. *Nature*, **416**, 389–395.

Watson CS (1996) The vegetational history of the Northern Apennines, Italy: information from three new sequences and a review of regional vegetational change. *Journal of Biogeography*, **23**, 805–841.

Webb RW, Rosenzweig CE, Levine ER (2000) Global soil texture and derived water-holding capacities. In: *Dataset*. Oak Ridge National Laboratory Distributed Active Archive Center, Oak Ridge, Tennessee, USA. Available at: http://www.daac.ornl.gov (accessed August 2000).

Zhu K, Woodall CW, Clark JS (2012) Failure to migrate: lack of tree range expansion in response to climate change. *Global Change Biology*, **18**, 1042–1052.

Supporting Information

Additional Supporting Information may be found in the online version of this article: